XIII ICSMFE, 1994, New Delhi, India / XIII CIMSTF, 1994, New Delhi, Inde

ISOTROPIC STRESS PROBING OF RECONSTITUTED SOILS

ESSAIS DU CHARGEMENT ISOTROPIQUE DE SOLS RECONSTITUES

J. Boháč

Institute of Theoretical and Applied Mechanics
Academy of Sciences of the Czech Republic
Prague, Czech Republic

SYNOPSIS: Experiments with reconstituted sand, loess and a sandy clay were carried out in a conventional and in a true triaxial apparatus. The specimens were isotropically compressed and swelled by small isotropic probes ($\delta\tau_{oct}=0$, $\delta\sigma_{oct}=25$ kPa) at $\tau_{oct}=0$ and at $\tau_{oct}=\pm 10$ kPa. The observed strain anisotropy of the specimens during isotropic loading depends on the full stress history of the soil. A threshold stress of about 7 times the previous stress was needed for erasing the recorded history. If an elasto-plastic model with a plastic potential surface is assumed, the strain anisotropy during isotropic loading could be reflected by kinematic plastic potential rather than by the plastic potential with a corner on the axis $\tau_{oct}=0$.

INTRODUCTION

It is well known that soils with anisotropic structure deform anisotropically when loaded by isotropic stress. In this way, the stress history (e.g. geological history or preparation of the specimen) recorded in the structure of the soil is reflected. However, there is a threshold state of stress at which the history is erased and the soil adapts to the new stress conditions.

If the soil is assumed elasto-plastic and normality condition is valid, the anisotropy can be described in plastic strains by the angle α

$$\alpha = \operatorname{atan}\frac{\frac{1}{2}\delta\gamma^{p}_{oct}}{\delta\varepsilon^{p}_{oct}} \qquad (1)$$

where $\delta\varepsilon_{oct}{}^{p}$ and $\delta\gamma_{oct}{}^{p}$ are the plastic increments of the normal and shear octahedral strains. According to normality criterion, the equation (1) identifies the shape of the plastic potential. For isotropic loading (1) gives the angle of intersection of the plastic potential with the axis $\tau_{oct}=0$ in the plane $\tau_{oct}:\sigma_{oct}$ superimposed by $\frac{1}{2}\delta\gamma_{oct}{}^{p}:\delta\varepsilon_{oct}{}^{p}$ (τ_{oct} and σ_{oct} are octahedral shear and normal stresses).

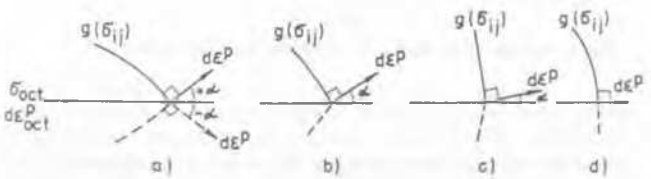

Fig 1 Definition of α and of a corner on plastic potential

For $\delta\gamma_{oct}{}^{p}\neq 0$ during isotropic loading ($\tau_{oct}=0$), the plastic potential is not perpendicular to the axis $\tau_{oct}=0$. If the plastic potential is to be symmetric around this axis, a corner (point of singularity) arises (Fig.1). The existence of the corners on plastic potentials was theoretically analyzed in Boháč and Feda (1991).

Another way of reflecting this anisotropy in the shape of the plastic potential is its rotation as in Fig.2 (kinematic plastic potential), or the plastic potential can have an irregular shape, being fitted to the experimental data.

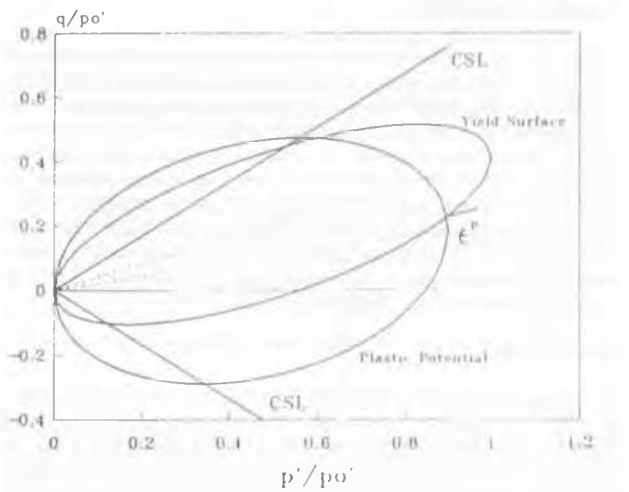

Fig 2 Kinematic plastic potential (after Davies and Newson, 1992)

In the paper, anisotropy of reconstituted specimens of four soils during isotropic loading is experimentally investigated both in total and in plastic strains. The objective was to find the magnitude of the stress needed for suppressing the anisotropy of the specimens structure and to identify the shape of the plastic potential at $\tau_{oct}=0$. All stresses are effective.

EXPERIMENTS

Equipment

The tests were carried out in a standard conventional triaxial cell (specimens of diameter 38 mm), hydraulic triaxial cell (38 mm), and in the true triaxial apparatus (cube 60 mm). In the standard triaxial apparatus axial strains were measured externally, using the proving ring to detect contact with the specimen. As only hydrostatic pressure was applied the external measurement of axial strains was not influenced by compliance effects and was deemed satisfactorily accurate.

Hydraulic triaxial system (Atkinson et al., 1985) with Hall effect transducers for local measurement of axial deformation was used for tests S1/92, S2/92, S3/92 and BE1. Volume changes were measured by IC gauge fitted with an LVDT, external axial deformation by LVDT.

The true triaxial apparatus (the cube) was based in principle on the cell by Ko and Scott (1967), with flexible membranes on each face of the prismatic sample of dimensions 60x60x60 mm. Axial strains in the centre of each face were measured by an LVDT and volume strains by IC gauge, but in processing the data the readings of axial transducers were used instead (nonuniformity of deformation, Abbis and Lewin, 1990). Since relatively small strains were measured during the probes, the nonuniformity of the deformation of the cube faces was supposed negligible.

Tested Soil

Two sands and two cohesive soils were tested. Zbraslav sand (tests denoted Z) is a medium quartzy sand with 50% of grains in the range 0.1 to 0.5 mm and 40% of grains 0.1 to 1 mm; $e_{max}=0.845$, $e_{min}=0.529$. Gabčíkovo sand (tests G) is a fine micaceous sand of grey colour, with organic admixtures and 15% of grains smaller than 0.06 mm; $e_{max}=0.923$, $e_{min}=0.639$. Both sands were sieved on 2 mm sieve before testing. Sedlec loess (tests S) has 70% of particles in the range 0.005 to 0.06 mm, $w_P=16\%$, $w_L=36\%$. Brickearth (tests B) from Rickmansworth is a sandy clay of $w_P=18\%$, $w_L=38\%$.

Specimen Preparation

All specimens were reconstituted and were tested in saturated state. Sand specimens were prepared in a split mould and mildly densified in layers by rodding. Brickearth for both triaxial and cube specimens was K_0-consolidated, in a floating ring consolidation press, from the slurry with the moisture content above w_L. Loess specimens were cut from a monolith prepared from the slurry ($w>w_L$) by K_0-consolidation (series SK_0). Six specimens (series SV) were cut from the monolith which was after K_0-consolidation subjected to vibrations on a shake table with the aim to rebuild its structure gained during K_0-consolidation. With all specimens the vertical consolidation pressure was about 100 kPa. No measures were taken to decrease the end restraint.

Test Procedure

Two kinds of loading were applied in triaxial cells. The first one was the isotropic compression (up to the effective pressure 600 to 1000 kPa depending on the applied back pressure) and swelling to the initial isotropic stress 120 kPa. In the standard triaxial cell the loading was carried out in steps σ_{oct}=25 kPa. In the hydraulic cell, specimens were loaded by isotropic pressure in a constant rate. The maximum permissible rate of loading was computed from the initial isotropic consolidation sequence.

The second path, carried out in the hydraulic apparatus, started also after the initial isotropic consolidation by 120 kPa. After the consolidation small isotropic probes ($\delta\tau_{oct}=0$) were applied from starting points both on the axis $\tau_{oct}=0$ and from points with $\tau_{oct}=\pm 10$ kPa. In the cube, similar probes were applied. Two specimens (TTBE1 and TTBE2) were K_0-consolidated before probing, specimen TTBE3 was consolidated isotropically and probed only on the axis $\tau_{oct}=0$.

In processing the data of the tests with medium Zbraslav sand, membrane penetration was taken into account according to Boháč and Feda (1992). In the case of tests with fine grained soils no correction for membrane penetration was made. Plastic strains were computed by subtracting recoverable strains obtained by unloading from the total ones.

RESULTS

Altogether 37 tests were evaluated. 17 tests were carried out with Zbraslav sand, 3 with Gabčíkovo sand, 13 with loess and 4 with brickearth (3 in the cube).

Degree Of Anisotropy

Typical data obtained from the stepwise isotropic compression are presented in Fig.3 and Fig.4., where $3\varepsilon_a$ is plotted against ε_v. It can be seen that experimental lines are concave, only test SV7 gave a more or less linear relationship $3\varepsilon_a:\varepsilon_v$, similarly like the rest of the tests with "vibrated" specimens of series SV (6 tests). Specimens SV had roughly

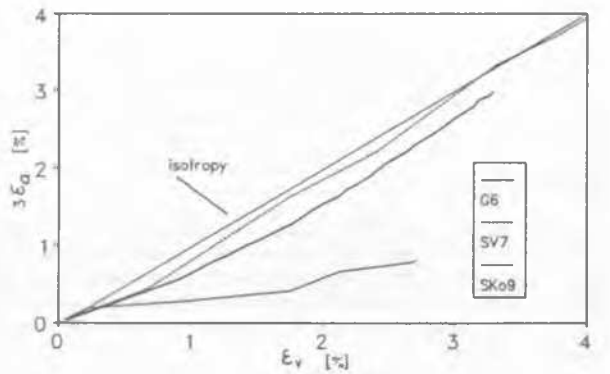

Fig 3 Examples of data from isotropic compression (loess and Gabčíkovo sand)

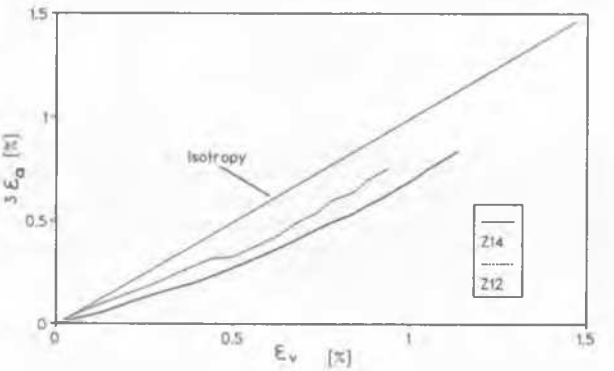

Fig 4 Results from isotropic compression (Zbraslav sand)

isotropic structure. This is not true with the specimens of series Z, G and SK_0 (without vibrations prior testing). The initial part of the diagrams $3\varepsilon_a:\varepsilon_v$ often has the direction $2\varepsilon_a:\varepsilon_v$ (G6, SV7 in Fig.3, Z14 and Z12 in Fig.4). Some specimens deformed at the beginning of compression even with $\varepsilon_a=\varepsilon_v$, i.e. they followed K_0-path. In the further stages, when the lines are concave, the increase of the radial stiffness is higher than that of axial stiffness, $\delta\varepsilon_a>\delta\varepsilon_r$ (ε_r is the radial strain). With isotropic pressure σ_{oct} increasing, $\delta\varepsilon_a\rightarrow\delta\varepsilon_r$. In this way, specimens undergo two stages of anisotropy with the axis of anisotropy rotated by 90°, although the overall behaviour can still be roughly isotropic.

Similar observations were reported by Ishihara (1984), who found that triaxial specimens of a sand did not deform laterally in the beginning of the tests. This is, surprisingly, in agreement with the tests of series SV (loess). It seems that this behaviour is not caused by parasitic effects during triaxial testing, since both bedding and end restraint should result in $\varepsilon_a > \varepsilon_r$ in the beginning of tests, followed by $\delta\varepsilon_r > \delta\varepsilon_a$, contrary to the results.

With all the tests the overall deformation process can be divided into three parts. In the initial one the structural skeleton is stiffer in the axial direction, specimen exhibits higher radial strains. In the second stage the skeleton is stiffer laterally. In the third stage, with the isotropic stress increasing, specimen adapts its structure due to isotropic stress applied and the structure becomes isotropic. Thus, in the deformation process a sequence of partial processes, caused by internal inhomogeneity of specimens can be distinguished with individual stiffness thresholds (Guyon, 1989). Investigation of the phenomena (so called effect of disorder, e.g. Ammi et al., 1989) seems, however, to be still at the first stage of analyzing two-dimensional arrays of particles.

Plastic Strain Increments

Each stress probe consisted of a closed cycle of loading and unloading. Elastic (recoverable) strains observed during unloading stage were subtracted from the total ones in computing the plastic strains. Deformations of reconstituted loess and brickearth were elasto-plastic, about 20 to 30% from the total strains being recoverable. With both tested sands roughly 50% of total strains were recoverable.

The anisotropy of the specimens can be expressed in plastic strains by the angle α defined by (1). For $\alpha = 0$ the soil is isotropic, $\alpha < 0$ indicates anisotropy with the stiffness higher in the axial direction, $\alpha > 0$ means higher stiffness in the radial direction. The equation (1) gives also the angle of intersection of the plastic potential with the axis $\tau_{oct} = 0$ in the plane $\tau_{oct}:\sigma_{oct} = 0$ (Fig.1). According to the above discussion of the results, $|\alpha|$ should decrease with the isotropic stress increasing and specimen becoming isotropic. Finally, when the specimen forms isotropic structure, $\alpha = 0$, Fig.1.

Tests in the standard triaxial apparatus

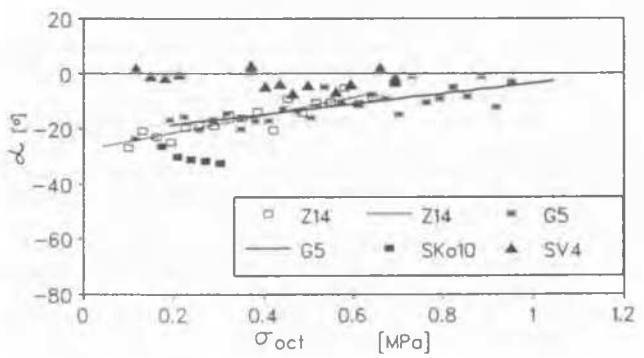

Fig 5 Typical dependence of α on σ_{oct} for tested soils

Typical dependence of α on σ_{oct} is in Fig.5. Data of individual tests were statistically evaluated and significant correlations between α and σ_{oct} were found. Examples of regression straight lines are shown in Fig.5 for tests Z14 and G5.

The tests depicted in Fig.5 characterize behaviour of each from the four series of tests. For series Z (Zbraslav sand) a dependence of α on σ_{oct} was found for each test, e.g. Z14 in Fig.5. From them, the overall relation for the series Z was found

$$\alpha[^\circ] = 31.7\sigma_{oct}[MPa] - 17.1 \qquad (2)$$

From (2), the stress needed for specimens Z to reach strain isotropy can be computed, σ_{oct} ($\alpha = 0$) $\doteq$0.54 MPa.

Corresponding value for series G (Gabčíkovo sand, more compressible than Zbraslav sand, with $\lambda = 0.022$ in comparison with $\lambda = 0.009$ of Zbraslav sand) $\sigma_{oct}(\alpha = 0) \doteq 1.22$ MPa can be obtained from

$$\alpha[^\circ] = 18.7\sigma_{oct}[MPa] - 21.8 \qquad (3)$$

If an elasto-plastic model is adopted for these soils, the plastic potential surface should intersect the axis $\tau_{oct} = 0$ in the angle $90^\circ - \alpha$, i.e. 76° and 70° for Zbraslav sand and Gabčíkovo sand respectively. Since for all data of the series Z and G $\alpha < 0$, the plastic potential does not have a corner on the $\tau_{oct} = 0$ axis (Fig.1) and could be rotated towards K_0-line as in Fig.2. With σ_{oct} increasing α decreases and for the stress computed from (2) and (3) there is only volumetric plastic strain, $\delta\gamma_{oct}^{pl} = 0$. The plastic potential is then perpendicular to the axis $\tau_{oct} = 0$.

For series SV (reconstituted loess, vibrated before testing) the value of α is approximately zero from the start of the isotropic compression (Test SV4 in Fig.5). Plastic potential intersects $\tau_{oct} = 0$ axis at 90°. No plastic shear strain occurs, the soil is isotropic.

This is not the case with series SK_0 (Test $SK_0$10 in Fig.5). The specimens were prepared by K_0-consolidation and were not vibrated before testing. They kept their cross-anisotropic structure during the tests. The range of the applied stress in this series is only 120 to 400 kPa, but test S1/92 carried out in hydraulic triaxial cell supports the results of the series SK_0. Hall effect transducers were used for local measuring of axial deformations and their data seem indicate that strain isotropy could be reached at about 700 to 800 Mpa (Fig.6). This is about $7\sigma_{oct,0}$ (the initial consolidation stress). For series SK_0 the average initial value ($\sigma_{oct} = 120$ kPa) $\alpha = -22^\circ$ and it is constant up to 400 kPa. In this range,

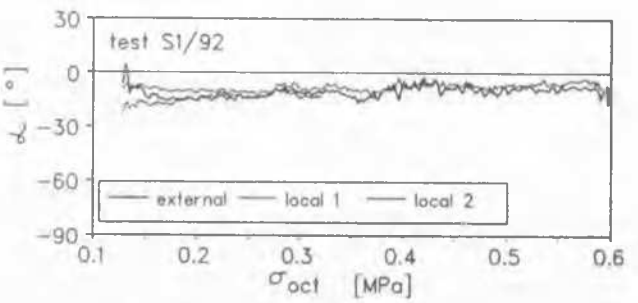

Fig 6 A test with loess in the triaxial apparatus, dependence of α on σ_{oct}

the plastic potential intersects the axis $\tau_{oct} = 0$ at a sharper angle than the other tested soils. However, the specimens differ in initial void ratio, $e_0 = 0.71$ for the series SK_0 and $e_0 = 0.52$ with test S1/92.

Tests in the hydraulic triaxial apparatus

Raw data from isotropic compression and swelling of the specimen S1/92 are in Fig.6. Similar data were obtained for brickearth specimen subjected to the same stress path, the average $\alpha = -15^\circ$. During the two other tests with loess, small isotropic probes of $\delta\sigma_{oct} = 25$ kPa were applied from starting points $\tau_{oct} = 0$ or $\tau_{oct} = \pm 10$. The paths between individual probes were either continuous isotropic compression or shearing $\delta\sigma_{oct} = 0$. In Fig.7, obtained plastic strains increment are plotted

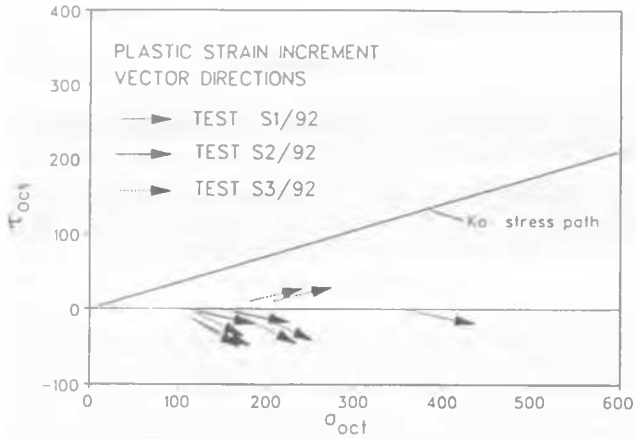

Fig 7 Results from the hydraulic cell, probes on loess specimens

from their starting points. The average values of α are: $\alpha = -13°$ for $\tau_{oct} = 0$, $\alpha = -21°$ for $\tau_{oct} = -10$ kPa and $\alpha = 11°$ for $\tau_{oct} = +10$ kPa. This means again that during isotropic compression plastic shear strains arose, which verifies the results obtained by testing in the standard triaxial cell. For the soil tested, plastic potential could be either rotated slightly towards K_0-axis, or, rather, a curve can be sketched in Fig.7 without stipulating any axis of symmetry.

Tests in the cube

In the cube three specimens of brickearth were tested. Specimens TTBE1 and TTBE2 were after setting up into the cell K_0-consolidated and probes were made after drained shearing ($\delta\sigma_{oct} = 0$) on the $\tau_{oct} = 0$ axis and directly on the K_0-path. The strain increments are plotted in Fig.8. From

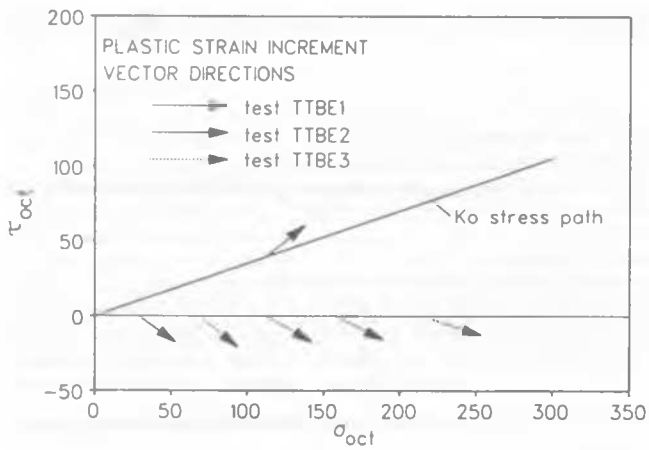

Fig 8 Tests on brickearth in the cube

five probes on the axis $\tau_{oct} = 0$ average $\alpha = -27°$, on the K_0-line $\alpha = 36°$. The plastic potential does not seem centred around either K_0 or $\tau_{oct} = 0$ axis.

CONCLUSION

Strains of the reconstituted specimens prepared by K_0-consolidation were anisotropic during isotropic compression. Sandy specimens with a compression structure induced by specimen preparation deformed also anisotropically. The observed anisotropy of reconstituted soils in isotropic loading was substantially higher than reported by Lewin (1973), α down to -27° in comparison with about -5° in Lewin (1973).

Specimens of the more compressible sand were more anisotropic than those of the stiffer one, though the preparation procedure was identical. Vibrating the K_0-consolidated monolith before cutting the specimens suppressed the original cross-anisotropic structure and the specimens behaved isotropically from the beginning of isotropic compression. The degree of anisotropy depends on the full previous stress path (recorded history) including the sample preparation (or geological history).

The magnitudes of the isotropic stress needed for adapting the structure of the tested sands were 600 kPa and about 1200 kPa, for less and more compressible sand respectively. The threshold for reconstituted loess was about 7 times the vertical stress during specimen preparation.

If an elasto-plastic constitutive model with a plastic potential is adopted for the tested soils, the structural cross-anisotropy, resulting in anisotropic strains during isotropic loading, should be reflected in the shape of plastic potential. For the reconstituted brickearth plastic potential does not have a corner on the plastic potential for $\tau_{oct} = 0$. Strain anisotropy is expressed by kinematic plastic potential rotated towards the previous stress path (K_0-path in Fig.8). For reconstituted loess the vectors in Fig.7 seem to indicate a corner. However, since during isotropic loading all values $\alpha < 0$, smooth curve without a point of singularity is more plausible.

ACKNOWLEDGEMENT

The research was partially supported by the grant 27114 of the Czechoslovak Academy of Sciences. Special thanks are due to Prof. J.H. Atkinson, director of GERC, City University, London, for making the facilities available for testing during the author's stay in London.

REFERENCES

Abbis, C.P. and Lewin, P.I. (1990), A test of the generalized theory of visco-elasticity in London Clay. Géotechnique, Vol. 40, No. 4, 40-57.

Ammi, M., Bideau, D., Messager, J.C., Travers, T. and Troadec, J.P. (1989), Compression of granular media: effects of disorder. In: Biarez, J. and Gourves, R. (ed.): Proc. Int. Conf. Micromech. Gran. Media "Powders and Grains", Balkema, 195-200.

Atkinson, J.H., Evans, J.S. and Scott, C.R. (1985), Developments in stress path testing equipment for measurements of soil parameters. Ground Engineering, Vol. 18, No. 1, 15-22.

Boháč, J. and Feda, J. (1991), Angularita plastického potenciálu zemin (Angularity of the plastic potential of soils - in Czech). To be published in Stavebnícky časopis, Bratislava.

Boháč, J. and Feda, J. (1992), Membrane penetration in triaxial tests. Geotechnical Testing Journal ASTM, Vol. 15, No. 3, 288-294.

Davies, M.C.R. and Newton, T.A. (1992), A critical state constitutive model for anisotropic soil. Proc. Wroth Memorial Symposium, Oxford, 128-134.

Guyon, E. (1989), The large disorder of granular matter. In: Biarez, J. and Gourves, R. (ed.): Proc. Int. Conf. Micromech. Gran. Media "Powders and Grains". Balkema, 17-20.

Ishihara, K. (1984), Data basis. In: Gudehus, G. et al. (ed.): Constitutive relations for soils. Balkema, 451-452.

Ko, H.-Y. and Scott, R.R. (1967), A new soil testing apparatus. Géotechnique, Vol.17, 40-57.

Lewin, P.I. (1973), The influence of stress history on the plastic potential. In: Palmer, A.C. (ed.): Proc. Symp. on Role of Plasticity in Soil Mechanics, Cambridge, 96-106.